



# Enhancement of glass-forming ability and bio-corrosion resistance of Zr–Co–Al bulk metallic glasses by the addition of Ag

C. Zhang, N. Li, J. Pan, S.F. Guo, M. Zhang, L. Liu\*

State Key Laboratory of Material Processing and Die & Mould Technology, Huazhong University of Science and Technology, 430074 Wuhan, China

## ARTICLE INFO

### Article history:

Received 26 July 2009

Received in revised form 2 February 2010

Accepted 10 February 2010

Available online 18 February 2010

### Keywords:

Metallic glasses

Rapid-solidification

Corrosion

Thermal analysis

## ABSTRACT

A novel Ni and Cu-free Zr-based bulk metallic glass (BMG) system with enhancement of glass-forming ability (GFA) and bio-corrosion resistance was prepared by copper mold casting by the addition of Ag. It was found that the addition of Ag can considerably enhance the glass-forming ability, as indicated by the increase of the critical glass dimension from 3 mm diameter of the ternary system to over 10 mm in the alloy of  $Zr_{53}Co_{18.5}Al_{23.5}Ag_5$ . The bio-corrosion behaviors of the Zr-based BMGs in phosphate buffered solution (PBS) were investigated by electrochemical polarization at 310 K. It was found that the addition of appropriate amount of Ag can enhance the corrosion resistance of the BMGs. The X-ray photoelectron spectroscopy (XPS) indicated that the formation of an  $Al_2O_3$ -enriched passive film is mainly responsible for the high corrosion resistance of Ag-bearing alloy in phosphate buffered solution.

© 2010 Elsevier B.V. All rights reserved.

## 1. Introduction

Zr-based bulk metallic glasses (BMGs) have attracted much attention in last decades due to their high glass-forming abilities (GFAs) and unique combination properties of superior strength (above 1.5 GPa), high elastic strain limit (around 2%), relatively low Young's modulus (50–100 GPa) and excellent corrosion resistance in phosphate buffered solution (PBS) [1–5]. The properties together with easy forming ability in the supercooled liquid region make the BMGs promising as biomaterials. However, most Zr-based BMGs developed up to date contain the elements of Ni and Cu, which are toxic to human body. Especially, Ni is usually blamed for the occurrence of an allergy and has antiproliferative effects on cell cultures [6]. To overcome the drawback, researchers have recently developed a few Ni-free Zr-based BMG systems including Zr–Cu–Fe–Al [1], Zr–(Cu, Ag)–Al [7,8], Zr–Co–Al–(Cu) [9,10], Zr–Cu–Pd–Al–Nb [11], Zr–Cu–Al [12] and Zr–Cu–Al–Ti [13]. Among them, the Zr–Co–Al BMGs are free of both Ni and Cu, thus are more promising to be biomaterials from the biocompatible point of view. However, the ternary Zr–Al–Co system suffers from poor glass-forming ability with a glassy diameter no more than 3 mm [9,10]. Until recently, the large size of BMG up to 18 mm in diameter was cast in  $Zr_{56}Al_{16}Co_{28}$  system with a near-eutectic composition [14].

It has been recently reported that addition of Ag can remarkably enhance the GFA and mechanical properties of some Zr-based sys-

tems. For instance, the addition of 2 at% Ag into Zr–Cu–Al system could increase the critical glassy diameter up to 12 mm from the original 5 mm [15]. More recently, Jiang et al. [7] reported that partial substitution of Cu by Ag in the  $Zr_{46}Cu_{46}Al_8$  alloy increased the critical glassy dimension from original 5 mm to large than 20 mm in  $Zr_{45}(Cu_{4.5/5.5}Ag_{1/5.5})_{48}Al_7$ . This modified alloy also owns very attractive mechanical properties with compressive yield stress of 2100 MPa and plasticity of 28%. In this paper, Ag was also chosen as the doped element in Zr–Co–Al system. It is shown that appropriate substitution of Ag for Co can considerably enhance the glass-forming ability of the ternary alloy. To investigate the biocompatibility of the Ni-free and Cu-free BMG, the corrosion resistance of the Ag-modified BMG was tested in artificial body fluid by electrochemical polarization measurement.

## 2. Experimental procedure

The alloy ingots with nominal composition of  $Zr_{53}Co_{23.5-x}Al_{23.5}Ag_x$  ( $x=0, 1, 3, 5, 7, 9$  at%) were prepared from elemental metals of pure Zr, Co, Al, Ag (purity > 99.5%) by arc-melting under a Ti gettered Ar atmosphere. The ingots were remelted at least five times to ensure chemical homogeneity. From the master alloys, sample rods with different diameters from 3 to 10 mm were produced by copper mold casting. The structure of the as-cast alloys was examined by X-ray diffraction (XRD, Philips  $\chi$ Pert PRO) with Cu  $K\alpha$  radiation, and thermal behavior was investigated by differential scanning calorimetry (DSC, Perkin-Elmer DSC-7) and differential thermal analyzer (DTA, Perkin-Elmer DTA-7) in a flow of argon atmosphere at a heating rate of 20 K/min.

Electrochemical polarization was conducted in a three-electrode cell using a platinum counter electrode and a saturated calomel reference electrode (SCE). The whole cell was kept at 310 K throughout the test. The electrolyte used in the present study is (PBS, pH 7.4), which is of 8.0 g/L NaCl, 0.2 g/L KCl, 0.14 g/L  $NaH_2PO_4$ , and 0.2 g/L  $KH_2PO_4$ . Corrosion samples were obtained from BMG rods (3 × 5 mm) transverse to the long axis and were closely sealed with epoxy resin, leaving only a

\* Corresponding author. Tel.: +86 27 87556894; fax: +86 27 87554405.

E-mail address: [lliu2000@mail.hust.edu.cn](mailto:lliu2000@mail.hust.edu.cn) (L. Liu).

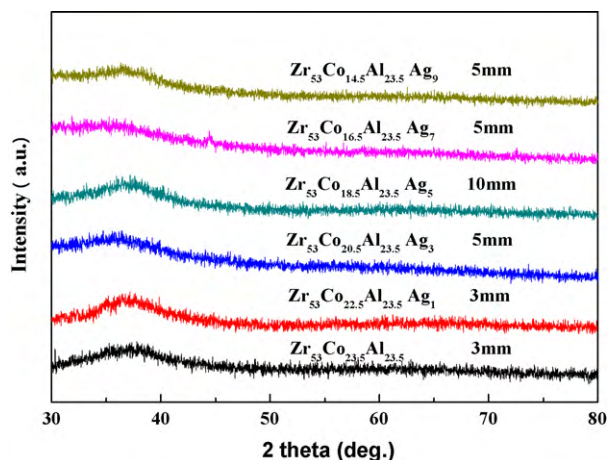


Fig. 1. XRD patterns of as-cast  $Zr_{53}Co_{23.5-x}Al_{23.5}Ag_x$  ( $x=0, 1, 3, 5, 7, 9$ ) bulk metallic glasses with different diameters.

longitudinal surface of about  $15\text{ mm}^2$  exposed for testing. The potentiodynamic polarization curves of the specimens were recorded at a potential sweep rate of  $1\text{ mV/s}$  when the open-circuit potential became almost steady after immersion in PBS for at least 20 min. To characterize the composition and chemical states of elements in passive film formed after electrochemical treatment, a specimen was potentiodynamically polarized nearly to the pitting potential and then taken out immediately for X-ray photoelectron spectroscopy (XPS, VGMultilab2000) analysis with  $Al\ K\alpha$  excitation. The binding energies of electrons were calibrated by the peak of C 1s, 284.8 eV. XPS spectra were analyzed by a least-squares fit with XPSPEAK analytical software to obtain further information about chemical status. In addition, galvanostatic-step technique (GIT) was applied to investigate the formation process of the passive film under a constant electrode current density of  $2\text{ mA/cm}^2$  at 310 K in PBS.

### 3. Results

Fig. 1 shows the XRD of as-cast  $Zr_{53}Co_{23.5-x}Al_{23.5}Ag_x$  ( $x=0, 1, 3, 5, 7, 9$ ) bulk metallic glasses with various diameters. As show in Fig. 1, the patterns of all samples consist of only broad diffraction hump without any Bragg peaks within the resolution limits of X-ray diffraction, indicating all alloys are fully amorphous structure in their respective dimensions. With Ag addition, the glass alloys with larger diameters have been prepared, and the best GFA is achieved for  $x=5$ , which has a critical diameter ( $d_c$ ) at least 10 mm. With further increase in Ag content, the  $d_c$  decreased to 5 mm for  $x=7$  and 9.

Fig. 2 shows the DSC and DTA curves of  $Zr_{53}Co_{23.5-x}Al_{23.5}Ag_x$  ( $x=0, 1, 3, 5, 7, 9$ ) BMGs with diameter of 3 mm. It can be seen that all BMGs exhibit a distinct glass transition followed by a wide supercooled liquid region before crystallization (see Fig. 2a). The glass transition temperature  $T_g$ , the onset crystallization temperature  $T_x$  and the supercooled liquid region  $T_x (=T_x - T_g)$  are listed in Table 1.  $T_g$  remains almost unchanged of about 770 K with different Ag contents, while the  $T_x$  decreases monotonously from 841 K for the Ag-free BMG to 821 K for the BMG containing 9 at% Ag, leading to the decrease of  $T_x$  from 69 to 52 K. On the other hand, the addition of Ag has a signification effect on the crystallization behavior of the mother alloy, as indicated by the change from a single-step crystal-

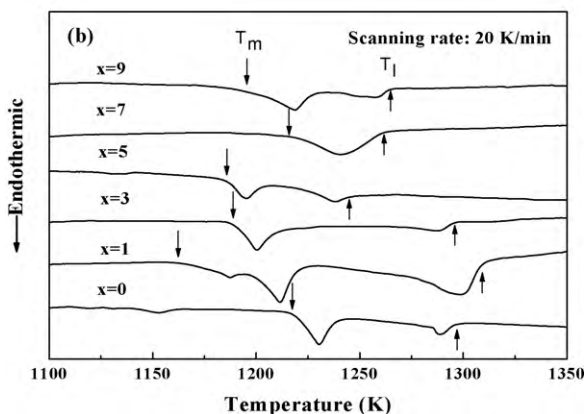
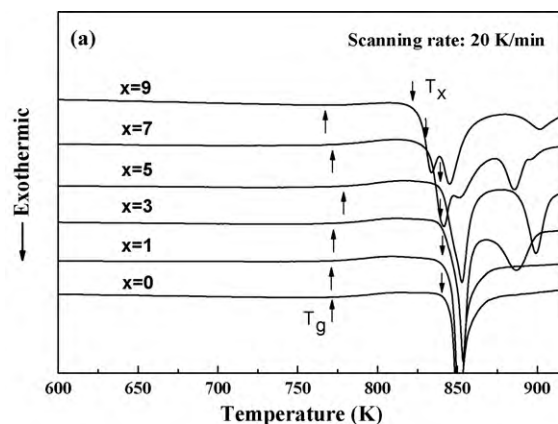


Fig. 2. DSC (a) and DTA (b) curves of the as-cast  $Zr_{53}Co_{23.5-x}Al_{23.5}Ag_x$  ( $x=0, 1, 3, 5, 7, 9$ ) alloys at heating rate of 20 K/min.

lization for the BMGs with  $x=0$  and 1 to a multi-step crystallization for the alloys with a higher content of Ag. The melting behavior of all the BMGs with various Ag contents is displayed in Fig. 2b, from which the melting temperature ( $T_m$ ) and liquidus temperature ( $T_l$ ) can be obtained and are also included in Table 1. As can be seen, the Ag content significantly affects  $T_l$  and the melting behavior of these glassy alloys. The base alloy has a high  $T_l$  of about 1296 K. With 5 at% Ag addition, the  $T_l$  value significantly decreases to 1185 K, which is the lowest in all BMGs, and then increases in the higher Ag content range. Additionally, there are multiple melting peaks for Ag-free BMG, indicating that the base alloy is at off-eutectic composition. As the Ag content increases, the melting peak in the high temperature range becomes smaller, and there is only a single melting peak for 7 at% Ag content, indicating that the  $Zr_{53}Co_{16.5}Al_{23.5}Ag_7$  alloy locates nearly at eutectic point.

Electrochemical polarization was conducted to study the bio-corrosion resistance of the BMGs in phosphate buffered solution, the samples with the Ag content of 0, 3 and 7 at% were chosen for exemplification. Fig. 3 shows the polarization curves of the BMGs in PBS open to air at 310 K and are compared to Ti–6Al–4V

Table 1

Summary of the critical sample diameters and the thermal parameters of  $Zr_{53}Co_{23.5-x}Al_{23.5}Ag_x$  ( $x=0, 1, 3, 5, 7, 9$ ) glass alloys.

$x$	$d_c$ (mm)	$T_g$ (K)	$T_x$ (K)	$\Delta T_x$ (K)	$T_m$ (K)	$T_l$ (K)	$T_{rg}$	$\gamma$	$\Delta H$ (J/g)
0	3	772	841	69	1217	1296	0.596	0.407	-51.5
1	3	771	840	69	1163	1309	0.589	0.404	-53.8
3	5	773	839	66	1189	1297	0.596	0.405	-55.4
5	10	776	839	63	1185	1245	0.623	0.415	-65.8
7	5	770	830	60	1215	1261	0.610	0.409	-52.9
9	5	769	821	52	1195	1265	0.608	0.404	-58.7

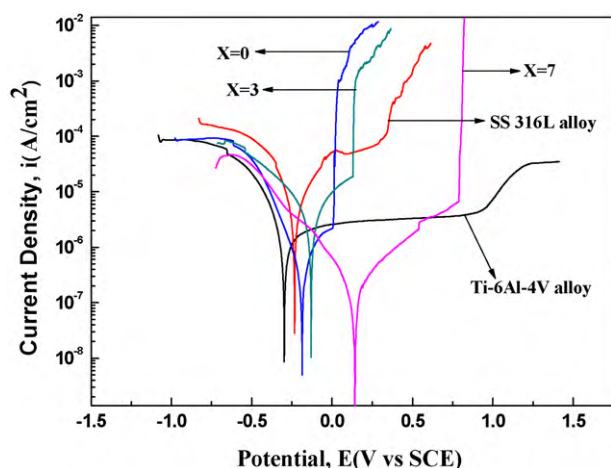


Fig. 3. Potentiodynamic polarization curves of  $Zr_{53}Co_{23.5-x}Al_{23.5}Ag_x$  ( $x=0, 3, 7$ ) BMGs in phosphate buffered solution open to air at 310 K.

alloy and 316L stainless steel. It can be seen that all BMGs show quite similar polarization behaviors in PBS, i.e. they were spontaneously passivated with very low passive current densities of the order of  $10^{-6}$  A/cm<sup>2</sup> and a distinct passive region before pitting. Among all BMGs, the one containing 7 at% Ag displays the highest corrosion resistance, as indicated by an extremely wide passive region of about 624 mV and the smallest passive current density of  $2.9 \times 10^{-7}$  A/cm<sup>2</sup>. Compared with 316L stainless steel, all BMGs show a superior corrosion potential with the passive current density of about one order of magnitude lower than 316L stainless steel, but comparable to Ti-6Al-4V alloy.

To better understand the corrosion mechanism of the BMGs in PBS, XPS was performed to characterize the composition and chemical status of elements in the passive film that was formed after potentiodynamic polarization in its passive region. For this purpose, the  $Zr_{53}Co_{16.5}Al_{23.5}Ag_7$  BMG which shows the highest corrosion resistance was chosen to be investigated and compared with the Ag-free BMG (i.e.  $Zr_{53}Co_{23.5}Al_{23.5}$ ). The XPS spectra of different elements are shown in Fig. 4a–e.

The Zr 3d spectrum consists of two peaks by multiplet splitting approximately at 182.0 and 184.3 eV, which can be assigned to Zr 3d<sub>5/2</sub> and Zr 3d<sub>3/2</sub> electrons originating from Zr<sup>4+</sup> oxide state (ox) [16]. The Al 2p spectrum was decomposed into three spectra peaked at 71.41 eV corresponding to Al 2p<sub>3/2</sub> electrons from metallic state (me), while at 74.45 and 75.50 eV Al 2p<sub>3/2</sub> electrons from Al<sup>3+</sup> oxide state [16]. The Ag 3d spectrum consists of two peaks at 368.3 and at 375.5 eV, which corresponds to Ag 3d<sub>5/2</sub> and Ag 3d<sub>3/2</sub> electrons originating from the metallic state [16]. The O 1s spectrum is fitted by two peaks, at 531.53–531.6 and at 533.3–533.5 eV assigned to OH<sup>-</sup> and to O<sup>2-</sup>, respectively. A broad peak corresponding to P<sub>2p</sub> spectrum appeared at 134.1 eV, which is attributed to PO<sub>4</sub><sup>3-</sup>. In addition, very little Co (about 0.3%) was detected in XPS, which is believed not to play a critical role in the outer passive film.

The atomic concentration of each element in the surface was calculated from the integrated intensity of the spectra, as summarized in Table 2. As can be seen, the proportion of phosphates increasing slightly and the Al oxides increasing drastically, while the concen-

tration of Zr oxides decreases considerably, with respect to the Ag-free alloy. The result implies that the improvement in corrosion resistance of Ag-bearing BMG should be closely related to the Al oxides and Zr oxides.

#### 4. Discussion

The experimental results demonstrate that the addition of appropriate amount Ag remarkably improved the glass-forming ability of the base alloy. Variation parameters,  $\Delta T_x$ , the reduced glass transition temperature  $T_{rg}$  ( $=T_g/T_l$ ) and  $\gamma$  ( $=T_x/T_g + T_l$ ) [13], are used to evaluate the GFA of the BMGs. From Table 1, one can notice that the  $Zr_{53}Co_{15.5}Al_{23.5}Ag_5$  BMG exhibits the largest  $T_{rg}$  of 0.623 and  $\gamma$  of 0.415, consistent with the largest critical size of 10 mm, demonstrating that this alloy has the highest GFA. The enhancement of the GFA of the BMGs by the addition of an appropriate amount of Ag can be well explained by Inoue's empirical rules and Egami's theory for easy glass formation. First, Ag is the second largest atom in the Zr–Co–Al–Ag system (Zr: 0.162 nm, Al: 0.143 nm, Co: 0.125 nm, Ag: 0.144 nm) with the atomic size ratio of Zr/Ag = 1.13 and Ag/Co = 1.15. The large discrepancy in atomic size of different constituents is beneficial to the formation of a dense atomic packing structure in melt and thus to the increase in GFA according to Inoue empirical law. Secondly, Ag has a negative heat of mixing with the major constituents of large atom radii in the system, e.g.  $-20$  kJ/mol for Zr–Ag and  $-4$  kJ/mol for Al–Ag, and other atomic pairs in the original ternary system have also a large negative heat of mixing. Although Ag has a positive heat of mixing with Co ( $+19$  kJ/mol), this repulsive interaction between Ag and Co may have possibly a positive effect on the GFA in the present system. Egami [17] pointed out that increasing the interaction between the small and large atoms would favor bulk metallic glass formation. Co has the smallest atom radii among the constituent elements, the repulsive interactions between Co and Ag will make Co atoms be more attracted by big atoms such as Zr and Al, so this confusion arrangement could reduce the mobility of Co atoms and, in turn, enhances the GFA. Similar phenomenon had been reported in our recent paper [18] in Zr–Cu–Fe–Al system, in which the addition of 3 at% Ag enhances significantly the glass-forming ability.

Finally, as know from DTA results, the liquidus temperature ( $T_l$ ) of the melt decreases with the increase in Ag content, and reaches the lowest value of 1245 K at 5 at%, this leads to a highest  $T_{rg}$  and  $\gamma$  for the  $Zr_{53}Co_{15.5}Al_{23.5}Ag_5$  BMG. The combination of big difference in atomic sizes, the large negative mixing heat values of main components and the significant reduction of liquidus temperature could stabilize the liquid state and increase the GFA of the system [19]. A similar result has been reported in Zr–Cu–Al–Ag system, for which the GFA increase considerably by the addition of Ag [7].

In addition, the results from electrochemistry polarization indicate that the addition of appropriate amount of Ag can also improve the corrosion resistance of the BMGs in PBS. XPS reveals that the addition of Ag can promote the formation of Al<sub>2</sub>O<sub>3</sub> but slightly suppressed the formation of ZrO<sub>2</sub>. In order to better understand the formation process of passive films of the BMGs with the addition of Ag, the kinetics for the formation of passive films with various Ag content ( $x=0, 3, 7$ ) was investigated by the galvanostatic-step test on anode at 310 K, as show in Fig. 5. It can be seen that the formation of the passive films of all the BMGs followed a one-step process with only one plateau of potential (i.e. the potential kept constant with the extension of anodizing time). Usually, the level of the potential plateau reflects the stabilization of the passive film, while the slope of linear part in potential–time curve refers to the formation rate of passive film [20]. The results indicate that the addition of Ag does not affect the rate of the formation of passive films but only changes the stability of passive films. The  $Zr_{53}Co_{16.5}Al_{23.5}Ag_7$  BMG

Table 2  
Compositions (at%) and chemical states of the passive films<sup>a</sup>.

Alloys	Zr (ox)	Al (ox)	Al (me)	Ag (me)	Phosphate
$Zr_{53}Co_{23.5}Al_{23.5}$	62.58	4.14	5.89	0	27.39
$Zr_{53}Co_{16.5}Al_{23.5}Ag_7$	51.60	18.14	3.84	0.66	25.76

<sup>a</sup> me and ox represent metallic and oxide state, respectively.

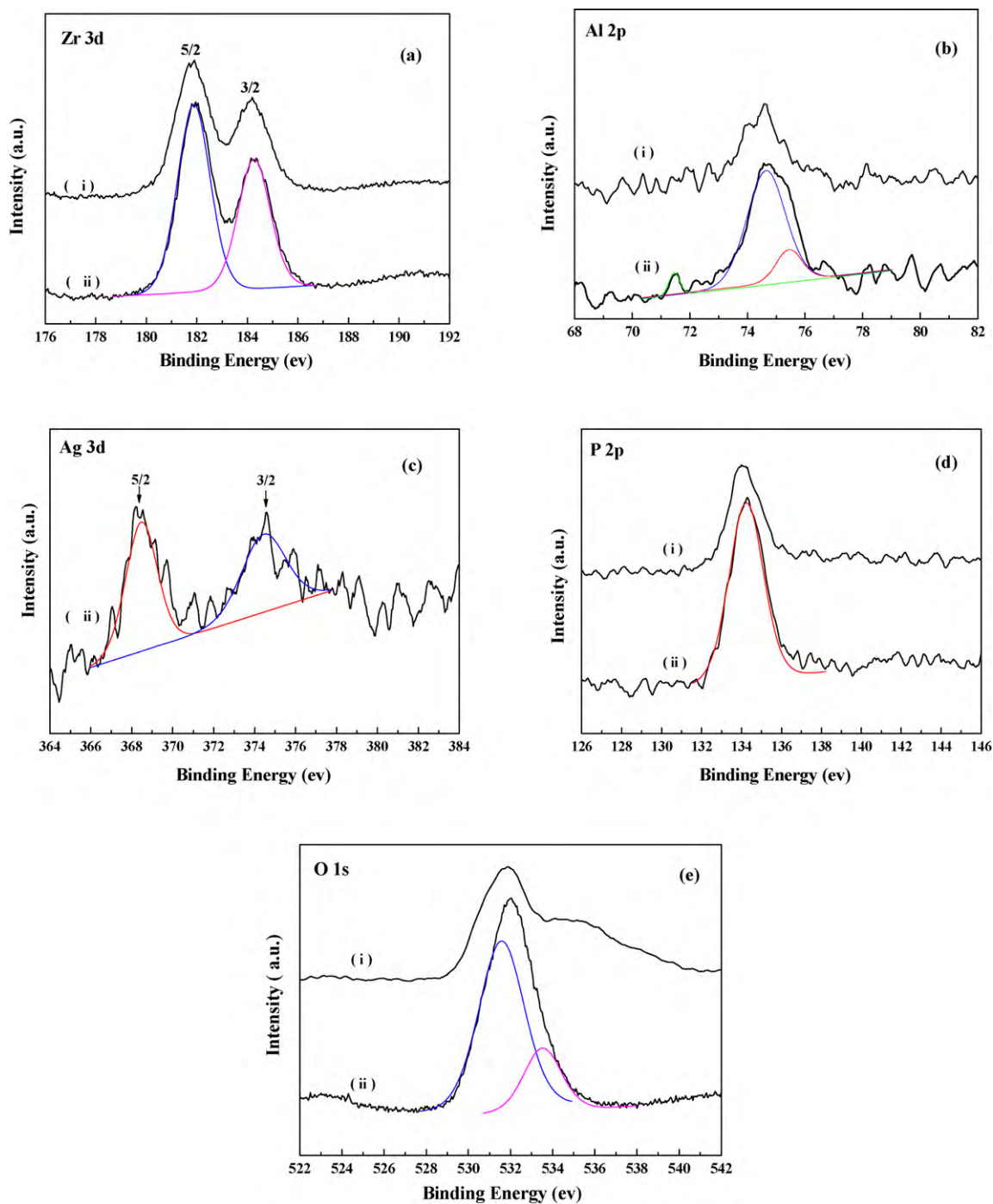


**Fig. 4.** XPS spectra of Zr 3d, Al 2p, Co 2p, O 1s electrons of BMGs without Ag and with 7 at% Ag: (a) Zr 3d; (b) Al 2p; (c) Ag 3d; (d) P 2p; (e) O 1s. (i)  $Zr_{53}Co_{16.5}Al_{23.5}$  alloy; (ii)  $Zr_{53}Co_{16.5}Al_{23.5}Ag_7$  alloy. The black curves represent raw XPS spectra, and the colored one fitted curves. (For interpretation of the references to color in this figure legend, the reader is referred to the web version of the article.)

shows the highest steady potential among all BMGs, demonstrating that the BMG exhibits a best corrosion resistance in PBS, which is well consistent with the polarization result.

It has been reported previously that the high-corrosion resistance of the Ag-doped Cu–Zr–Ag–Al glass alloys is attributed to their single glass phase nature and formation of  $Zr^{4+}$ - and  $Al^{3+}$ -enriched oxide surface film in the corrosive solutions [21,22]. XPS analysis revealed that the oxides formed on the sample surface consist mainly of  $ZrO_4$  and  $Al_2O_3$  for both Ag-free and Ag-bearing BMGs, as shown in Table 2. As compared with the Ag-free BMG, the addition of Ag increases significantly the amount of  $Al_2O_3$ , but

slightly decreases the amount of  $ZrO_4$ . Although the two kinds of oxides are of a dense, compact and stable structure, and have a highly protective ability against corrosion. However, in the simulated body fluid, containing both chloride ion and phosphate ion,  $Al_2O_3$  is more protectable than  $ZrO_2$ . Because Zr oxides are prone to absorb phosphate ion ( $PO_4^{4-}$ ) [23,24], which, on the other hand, can be easily replaced by chloride ion and results in the increase of target for chloride ion and subsequently degrade the corrosion resistance of the alloy. Therefore, the less phosphate ion is, the better the corrosion resistance is. This comprises the reason for the improvement of corrosion resistance of the  $Zr_{53}Co_{16.5}Al_{23.5}Ag_7$

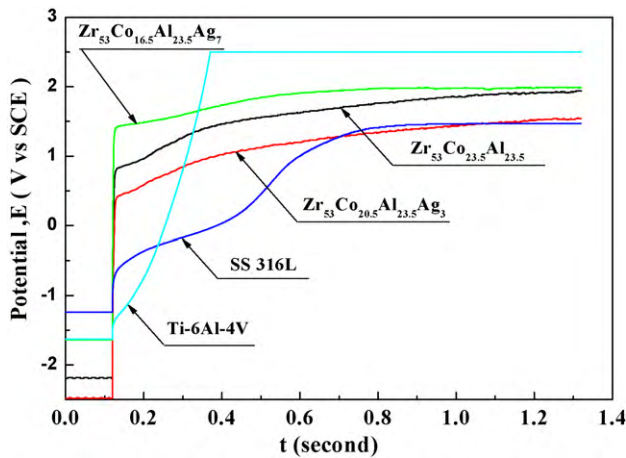


Fig. 5. The potential–time ( $E-t$ ) of  $Zr_{53}Co_{23.5-x}Al_{23.5}Ag_x$  ( $x=0, 3, 7$ ) alloys anodizing at  $2\text{ mA/cm}^2$  in PBS, at 310 K.

BMG as compared with the Ag-free BMG. However, the reason why Ag addition suppressed the formation of Zr oxides, but promote the formation of Al oxide is still unknown, which need more comprehensive investigations.

## 5. Conclusions

The addition of Ag to Zr–Co–Al ternary bulk metallic glasses greatly increases the stability of supercooled liquid with high value of  $T_{lg}$  and  $\gamma$ , leading to a significantly increases in the GFA. A fully glass alloy rod with a diameter of at least 10 mm was obtained in  $Zr_{53}Co_{15.5}Al_{23.5}Ag_5$  alloy. It is also revealed that the addition of appropriate amount of Ag (i.e. 7 at%) evidently improved the corrosion resistance of Zr-based BMGs in PBS. The improvement of corrosion resistance of is attributed to the fast formation of  $Al_2O_3$ -enriched passive film which is highly protectable to BMGs in PBS containing chloride ion and phosphate ion. The present results imply that the new Ni and Cu-free Zr-based BMGs are promising for biomedical use.

## Acknowledgements

This work was financially supported by Doctoral Program for Higher Education of China under Grant No. 200804870033 and by the Natural Science Foundation of China under Grant No. 50871042. This work was also partially supported by the Basic Research Foundation of National Universities, HUST (C2009Z018J). The authors are grateful to the Analytical and Testing Center, HUST, for technical assistance.

## References

- [1] K.F. Jin, J.F. Löffler, *Appl. Phys. Lett.* 86 (2005) 241909.
- [2] A. Inoue, *Mater. Trans. JIM* 36 (1995) 866.
- [3] L. Liu, C.L. Qiu, M. Sun, Q. Chen, K.C. Chan, G.-H. Pang, *Mater. Sci. Eng. A* 449–451 (2007) 193–197.
- [4] J.G. Wang, B.W. Choi, T.G. Nieh, C.T. Liu, *J. Mater. Res.* 15 (2000) 913.
- [5] Q.K. Jiang, X.P. Nie, Y.G. Li, Y. Jin, Z.Y. Chang, X.M. Huang, J.Z. Jiang, *J. Alloys Compd.* 443 (2007) 191–194.
- [6] J.C. Wataha, P.E. Lockwood, A. Schedle, *J. Biomed. Mater. Res.* 52 (2002) 360.
- [7] Q.K. Jiang, X.D. Wang, X.P. Nie, G.D. Zhang, H. Ma, H.-J. Fecht, J. Bendnarcik, H. Franz, Y.G. Liu, Q.P. Cao, J.Z. Jiang, *Acta Mater.* 56 (2008) 1785–1796.
- [8] W. Zhang, Q.S. Zhang, A. Inoue, *J. Mater. Res.* 23 (May (5)) (2008).
- [9] T. Zhang, A. Inoue, *Mater. Sci. Eng. A* 75–377 (2004) 432–435.
- [10] X.F. Zhang, Y.M. Wang, J.B. Qiang, Q. Wang, D.H. Wang, D.J. Li, C.H. Shek, C. Dong, *Intermetallics* 12 (2004) 1275–1278.
- [11] C.L. Qiu, Q. Chen, L. Liu, K.C. Chan, J.X. Zhou, P.P. Chen, S.M. Zhang, *Scripta Mater.* 55 (2007) 605.
- [12] A. Inoue, D. Kawase, A.P. Tsai, T. Zhang, T. Masumoto, *Mater. Sci. Eng. A* 178 (1994) 255.
- [13] J.B. Qiang, W. Zhang, G.Q. Xie, A. Inoue, *J. Non-Cryst. Solids* 354 (2008) 2054–2059.
- [14] T. Wada, F.X. Qin, X.M. Wang, M. Yoshimura, A. Inoue, N. Sugiyama, R. Ito, N. Matsushita, *J. Mater. Res.* 24 (2009) 2941–2948.
- [15] G.Q. Zhang, Q.K. Jiang, L.Y. Chen, M. Shao, J.F. Liu, J.Z. Jiang, *J. Alloys Compd.* 424 (2006) 176–178.
- [16] <http://www.lasurface.com/avantage/index.php>.
- [17] T. Egami, *J. Non-Cryst. Solids* 317 (2003) 30.
- [18] Z. Liu, K.C. Chan, L. Liu, *J. Alloys Compd.* 487 (2009) 152–156.
- [19] A. Inoue, A.R. Yavari, W.L. Johnson, R.H. Dauskardt, *MRS, Warrendale*, 2001, pp. L12.13.1–L12.13.6.
- [20] L. Liu, B. Liu, *Electrochim. Acta* 51 (2006) 3724–3730.
- [21] C.L. Qiu, W. Zhang, Q.S. Zhang, K. Asami, A. Inoue, *J. Mater. Res.* 23 (2008) 2091–2098.
- [22] W. Zhang, Q.S. Zhang, C.L. Qiu, A. Inoue, *Mater. Sci. Eng. B* 148 (2008) 92–96.
- [23] S. Hiroamoto, A.-P. Tsai, M. Sumita, T. Hanawa, *Corros. Sci.* 42 (2000) 1651–1660.
- [24] T. Hanawa, O. Okuno, H. Hamanaka, *J. Jpn. Inst. Met.* 56 (1992) 1168.